Online Supplemental Methods.

Animals, infection and treatment. We infected 39 mycobacteria-naive Indian rhesus macaques acquired from the TNPRC breeding colony supported by the NIH (Supplementary Table 1) with a low dose of *Mtb* CDC1551 via aerosol that developed asymptomatic LTBI infection with low detection of viable *Mtb* cfus in the BAL fluid and low serum C reactive protein (CRP) levels >3 μg/mL by 9 weeks post-infection with *Mtb*. Methods for aerosol infection with *Mtb* have been described in detail previously (1-6). A subset of 16 LTBI *Mtb*-infected rhesus macaques was co-infected with 300 TCID50 SIVmac239 intravenously at week 9 post-*Mtb* infection (Fig 1A). Of this subset, 7 had unperturbed *Mtb* infection post-SIV co-infection and were considered "Nonreactivators" (NR) while 9 were considered to be "Reactivators" (R) based on extensive clinical and microbiological evidence of TB disease in the post-SIV time-points (Fig 1B-K). A subset of 5 LTBI *Mtb*-infected rhesus macaques was co-infected with 300 TCID50 SIVmac239ΔGY intravenously at week 9 post-*Mtb* infection (Fig 1A). A subset of 8 LTBI *Mtb*-infected rhesus macaques was administered a macaque $CD4^+$ T cell-depleting antibody CD4R1 (50 mg/kg administered once every 2-3 weeks intravenously) obtained from the CD4R1 antibody provided by NHP Reagent Resource, Boston, MA, USA (Fig 1A). The depleting antibody was administered every two-three weeks (i.e., weeks 9, 11, 13, 15, 18) per the manufacturer's instructions. This antibody has been extensively used to deplete $CD4^+$ T cells in macaques (7, 8). The animals were

subjected to weekly physical examinations by board certified clinician(s), including body temperature and weight, and complete blood chemistries, including serum CRP evaluated.

Measurement of *Mtb* infection progression and TB disease. To measure the extent of TB disease following aerosol *Mtb* infection in the various groups of animals, we studied serum CRP levels weekly, as described (1-6, 9). Viable *Mtb* CFUs were obtained from BAL fluid at weeks 3, 7, 11, 15, 19, and from the lungs, bronchial lymph nodes, spleen, liver and kidney at necropsy, as described earlier (4-6). We also evaluated CFUs from individual lung granulomas isolated at necropsy, as described earlier (6, 10).

Measurement of SIV viral loads. Plasma viral loads (PVL) were measured in plasma collected from macaques infected with either the parental SIVmac239 or the SIVΔGY mutant using a PCR-based assay as described earlier (1, 6, 11).

Flow cytometry. Flow cytometry was performed on whole blood, BAL and lung samples from all animals, as previously described (4-6, 10, 12, 13). Blood and BAL were collected for flow cytometric analysis at week 3, 7, 11, 15, 19, and necropsy, depending on survival, to characterize T cell numbers, phenotype, proliferation and migration. At necropsy, PBMCs, BAL and lung cells isolated from each animal were stimulated to show changes in T cell functionality dependent upon disease state. Antibodies used for analysis of T cell populations included the following antibodies from BD Biosciences: CD3 (clone SP34-2), CD4 (clone L200), CD8 (clone RPA-T8), CD20 (clone 2H7), CD28

(clone CD28.2), CD69 (clone FN50), CD95 (clone DX2), HLA-DR (clone L243), Ki67 (clone B56), CCR5 (clone 3A9), CCR7 (clone 3D12), and PD-1 (clone EH12.2H7) (6, 10).

Confocal microscopy. Fluorescent immunohistochemistry, chromogenic staining, and *in situ* hybridization were performed on formalin-fixed, paraffin-embedded tissue as previously described (14).

RNA isolation. RNA was isolated using TRIzol™ Reagent (ThermoFisher Scientific Cat no: 15596018). BAL cells were resuspended with 1 mL of TRIzol reagent and lysed by pipetting. Lung tissue was isolated at necropsy and homogenized in a gentleMACS dissociator. Next, 200µl of chloroform was added to each tube and mixed well by shaking up and down. They were then centrifuged for 15 minutes at 12,000xg at 4°C and the upper aqueous layer was carefully collected. The RNA was precipitated by adding 1µl of glycogen (Invitrogen cat no: 10814010) and equal volume of isopropyl alcohol. Incubation at -20°C for 10 minutes was done and followed up by centrifugation at 12,000xg for 10 minutes at 4°C. Finally, the RNA pellet was washed twice with 500µl of 75% ethanol. The pellet was air dried and reconstituted in 30µl of RNase-free water. To remove the contaminating DNA, the samples were treated with TURBO™ DNase (ThermoFisher Scientific Cat no: AM2238) and RNA cleanup done using RNeasy Mini Kit (Qiagen) according to manufacturer's protocol. Finally, the concentration of the RNA samples was measured using Qubit 4 Fluorometer.

cDNA preparation. cDNA was prepared using RevertAid RT Reverse Transcription Kit (ThermoFisher Scientific cat no: K1691) according to manufacturer's protocol. Approximately 1μg of RNA was used per sample.

qRT-PCR. Quantitative SYBR Green-based qRT-PCR was performed with Applied Biosystems™ PowerUp™ SYBR™ Green Master Mix (Cat no: A25776). RT² Custom Profiler PCR Arrays (Qiagen Cat no: 330171) were used and the plate was loaded into an Applied Biosystem QuantStudio 5 Real-time PCR machine. The thermocycler was run with an incubation for 2 min at 50˚C, followed by an initial denaturation for 10 mins at 95˚C. The PCR stage program was set at 95˚C for 15 sec, followed by 60˚C for 1 min for 40 cycles. The PCR stage was followed by Melt curve stage according to equipment default conditions. 'ACTB' was used as the housekeeping gene to normalize expression levels, and the fold change was calculated using the comparative CT method.

Transcriptomics. Transcriptional differences between the animals with LTBI, active disease, SIVmac239-reactivation, SIVmac239-nonreactivation, SIVΔGY co-infection, and CD4-depletion were analyzed using *M. mulatta* (rhesus macaque) specific Agilent 4x44 DNA microarray reagent as described earlier (3-5, 15). Gene-enrichment analysis was performed using DAVID as described earlier. Within DAVID, various modalities were to perform gene-enrichment analyses including Gene Ontology (GO) Molecular Functions or Biological Processes (Fig 4A,D,E), Categories (Fig 4C), and INTERPRO

(Fig 4B). Output from DAVID utilized appropriate correction for repeated measures for multiple comparisons (Bonferroni).

Measurement of cytokine levels. We performed cytokine analyses on plasma and BAL supernatant using the Cytokine/Chemokine/Growth Factor 37-Plex NHP ProcartaPlex™ Panel (Invitrogen) according to the manufacturer's instructions and as described earlier for supernatants derived from macaque cells infected with *Mtb* (16).

Statistical analyses. Statistical comparisons were performed using one-way or two-way analysis of variance (ANOVA) in GraphPad Prism with Sidak's or Tukey's correction for multiple hypotheses, or one unpaired Students t-test as noted in figure legends as described previously (4). *P < 0.05; **P < 0.01; ***P < 0.001; ****P <0.0001. All figures are shown as mean ± SEM.

Study approval. All animal procedures were specifically approved by the Tulane National Primate Research Center Institutional Animal Care and Use Committee. All work related to biological containment was approved by the Tulane Institutional Biosafety Committee.

Author Contributions. A.N.B. developed the study design, carried out the experiments, analyzed the results, and participated in manuscript preparation; T.W.F., A.C. and X.A. carried out the experiments and analyzed some results; B.T. , M.G.K. and N.A.G. carried out the experiments; D.K.S. and T.H.L. analyzed some results; J.A.H. provided

vital reagents and helped with interpretation; J.R., S.M. and M.A helped with interpretation and participated in manuscript preparation; S.A.K. and D.K. developed the study design, analyzed the results, and participated in manuscript preparation.

Supplementary Table 1. Age, gender, and MAMU-type of each Indian rhesus macaque included in this study.

				Previous Publication	MAMU-Type									
Animal ID	Status	Age (Years)	Sex		A*01	A*02	A*08	A*11	B*01	B*03	B*04	B*08	B*17	DR2011
FE10	LTBI	7.00	MALE	PNAS 2016	-	+	-	-	-	-	-	-	-	-
FJ05	LTBI	6.81	MALE	PNAS 2016	+	+	-	-	+	-	-	-	-	-
GP50	LTBI	11.18	MALE	Tuberculosis 2019	+	-	-	+	+	-	-	-	-	+
HA90	LTBI	4.06	MALE	PNAS 2016	N/A	N/A	N/A	N/A	N/A	N/A	N/A	N/A	N/A	N/A
HB74	LTBI	4.07	MALE	PNAS 2016	+	-	-	-	-	-	-	-	-	+
HC90	LTBI	4.01	MALE	PNAS 2016	+	+	-	-	-	-	-	-	-	+
HV02	LTBI	9.34	MALE	Tuberculosis 2019	-	-	+	-	+	-	-	-	-	-
JD72	LTBI	7.38	MALE	Tuberculosis 2019	-	+	+	-	-	-	-	-	-	-
JF47	LTBI	7.32	MALE	Tuberculosis 2019	-	-	-	+	-	-	-	-	-	+
JN75	LTBI	5.45	MALE	Tuberculosis 2019	+	-	-	-	-	-	-	-	-	+
ER44	NR	8.61	MALE	PNAS 2016	-	-	-	+	-	-	-	-	-	-
HB12	NR	4.97	MALE	PNAS 2016	+	-	-	-	-	-	-	-	+	-
HV08	NR	3.85	MALE	PNAS 2016	+	-	-	-	+	-	-	-	-	-
ID01	NR	3.58	MALE	PNAS 2016	+	-	+	-	-	-	-	-	-	-
JF23	NR	7.26	MALE	Tuberculosis 2019	+	-	-	-	-	-	-	-	-	-
JH07	NR	7.32	MALE	Tuberculosis 2019	-	+	-	-	+	-	-	-	-	-
JI68	NR	6.06	MALE	Tuberculosis 2019	-	-	-	-	+	-	-	-	-	-
EH92	R	8.94	MALE	PNAS 2016	-	-	-	+	-	-	-	-	-	
HP22	R	3.79	MALE	PNAS 2016	+	+	-	-	-	-	-	-	-	+
HP41	R	3.78	MALE	PNAS 2016	-	-	-	-	+	-	-	-	-	-
ID91	R	3.67	MALE	PNAS 2016	+	-	-	-	+	-	-	-	-	-
IF04	R	3.53	MALE	PNAS 2016	-	-	+	-	-	-	-	-	-	-
IP88	R	7.05	MALE	Tuberculosis 2019	+	-	-	-	+	-	-	-	-	-
JE48	R	6.33	MALE	Tuberculosis 2019	-	+	-	-	-	-	-	-	-	-
KG40	R	5.51	MALE	Tuberculosis 2019	-	-	+	-	-	-	-	-	-	-
LE24	R	4.39	MALE	N/A	-	-	-	-	-	-	-	-	-	-
JF92	SIVΔGY NR	6.86	MALE	N/A	-	-	-	-	-	-	-	-	-	-
JN91	SIVΔGY NR	5.91	MALE	N/A	-	-	+	-	-	-	-	-	-	-
JT03	SIVΔGY NR	5.76	MALE	N/A	-	-	+	-	-	-	-	-	-	-
KB26	SIVΔGY NR	4.45	MALE	N/A	-	-	+	-	-	-	-	-	-	-
KK75	SIVΔGY NR	4.02	MALE	N/A	-	-	-	+	+	-	-	-	-	+
HP70	CD4R1-antibody	9.65	MALE	N/A	-	-	-	+	-	-	-	-	+	-
JC82	CD4R1-antibody	8.30	MALE	N/A	+	-	-	-	-	-	-	-	-	+
JT56	CD4R1-antibody	6.99	MALE	N/A	N/A	N/A	N/A	N/A	N/A	N/A	N/A	N/A	N/A	N/A
KC31	CD4R1-antibody	6.28	MALE	N/A	+	-		-	-	-	-	-	+	-
KE82	CD4R1-antibody	5.72	MALE	N/A	-	+	-	-	+	-	-	-	-	+
KH07	CD4R1-antibody	5.52	MALE	N/A	-	-	+	-	+	-	-	-	-	-
KH59	CD4R1-antibody	5.45	MALE	N/A	-	-	-	-	-	-	-	-	-	-
KN66	CD4R1-antibody	4.67	MALE	N/A	+	-	-	-	-	-	-	-	-	-

Supplementary Table 2. A list of genes which exhibited the most significantly differential expression in the lungs of the four groups of macaques (*Mtb*/SIV co-infected reactivators, *Mtb*/SIV co-infected nonreactivators, *Mtb*/SIVΔGY co-infected animals, and *Mtb* infected/CD4R1-administered animals (n=3 per group).

Gene.ID	Description	Av FC Nonreactivators	Av FC Reactivators	Av FC SIVDGY co-infected	Av FC CD4R1-ab	FDR corrected p-val
A_01_P008264	UBE2G1 ubiquitin conjugating enzyme E2 G1 [*Homo sapiens* (human)]	1.679650617	0	0	0	2.70E-13
A_01_P008438	TMEM132D transmembrane protein 132D [*Homo sapiens* (human)]	1.075006919	0	0	0	2.42E-11
A_01_P016609	SPANXA1 sperm protein associated with the nucleus, X-linked, family member A1 [*Homo sapiens* (human)]	1.938011776	0	0	0	5.81E-09
A_01_P003334	PREDICTED: Macaca mulatta transmembrane phosphoinositide 3-phosphatase and tensin homolog 2 (TPTE2), mRNA [XM_015120686]	1.221954473	0	0	0	8.51E-09
A_01_P009100	TTLL10 tubulin tyrosine ligase like 10 [*Homo sapiens* (human)]	1.845640839	0	0	0	1.25E-08
A_01_P006299	COL25A1 collagen type XXV alpha 1 chain [*Homo sapiens* (human)]	1.693527458	0	0	0	3.44E-08
A_01_P005542	F8A1 coagulation factor VIII associated 1 [*Homo sapiens* (human)]	2.122188732	0	0	0	6.39E-08
A_01_P011652		1.293673765	0	0	0	2.01E-07
A_01_P004402	KCNQ2 potassium voltage-gated channel subfamily Q member 2 [*Homo sapiens* (human)]	1.339743811	0	0	0	2.08E-07
A_01_P013786	MRAP melanocortin 2 receptor accessory protein [*Homo sapiens* (human)]	1.729281549	0	0	0	2.54E-07
A_01_P017611	C21orf62-AS1 C21orf62 antisense RNA 1 [*Homo sapiens* (human)]	0.967763143	0	0	0	3.39E-07
A_01_P003803	RNF145 ring finger protein 145 [*Homo sapiens* (human)]	-0.997523423	2.470752434	0.118019743	0.23124571	3.90E-07
A_01_P014060	KLRG2 killer cell lectin like receptor G2 [*Homo sapiens* (human)]	1.958272719	0	0	0	5.56E-07
A_01_P018664	CYP1A2 cytochrome P450 family 1 subfamily A member 2 [*Homo sapiens* (human)]	1.535634405	0	0	0	6.56E-07
A_01_P009355	WWOX WW domain containing oxidoreductase [*Homo sapiens* (human)]	2.341535428	0	0	0	7.17E-07
A_01_P017975	CD55 CD55 molecule (Cromer blood group) [*Homo sapiens* (human)]	-1.938041253	0.390481911	-1.771757462	-1.468369828	8.33E-07
A_01_P015936		-1.495028301	1.78144712	-0.026925705	0.129720193	9.82E-07
A_01_P009087	SYT2 synaptotagmin 2 [*Homo sapiens* (human)]	1.652394402	0	0	0	1.03E-06
A_01_P003758	potassium channel tetramerization domain containing 13 [Source:HGNC Symbol;Acc:HGNC:22234] [ENSMMUT00000062657]	1.225153081	0	0	0	1.04E-06
A_01_P009238	LARP6 La ribonucleoprotein domain family member 6 [*Homo sapiens* (human)]	-2.348993257	0	0	-1.390912227	1.13E-06
A_01_P016221		1.787258288	0	0	0	1.33E-06
A_01_P005857		1.655112909	0	0	0	1.39E-06
A_01_P018896	EPHA8 EPH receptor A8 [*Homo sapiens* (human)]	1.732330175	0	0	0	1.55E-06
A_01_P007576	LAMC3 laminin subunit gamma 3 [*Homo sapiens* (human)]	1.650775186	0	0	0	1.72E-06
A_01_P003339	IL36B interleukin 36 beta [*Homo sapiens* (human)]	1.523378984	0	0	0	1.80E-06
A_01_P016155	TACR1 tachykinin receptor 1 [*Homo sapiens* (human)]	1.78915129	0	0	0	1.82E-06
A_01_P000817	SEMA6B semaphorin 6B [*Homo sapiens* (human)]	0.704670267	0	0	-0.102448085	1.92E-06
A_01_P009147	ZC3H18-AS1 ZC3H18 antisense RNA 1 (head to head) [*Homo sapiens* (human)]	1.703551687	0	0	0	1.99E-06
A_01_P004080	RPP38 ribonuclease P/MRP subunit p38 [*Homo sapiens* (human)]	-2.818907521	0	0	0	2.16E-06
A_01_P002947	PPP2CA protein phosphatase 2 catalytic subunit alpha [*Homo sapiens* (human)]	-1.886692631	0	0	0	2.18E-06
A_01_P000690	STK32B serine/threonine kinase 32B [Homo sapiens (human)]	1.555930547	0	0	0	2.72E-06
A_01_P017341	REM2 RRAD and GEM like GTPase 2 [*Homo sapiens* (human)]	1.541066138	0	0	0	4.64E-06
A_01_P003684	IL10RB interleukin 10 receptor subunit beta [*Homo sapiens* (human)]	-1.610011716	2.208213686	0.011586729	0.422466279	5.10E-06
A_01_P006361	TSPYL5 TSPY like 5 [*Homo sapiens* (human)]	1.785668233	0	0	0	5.17E-06
A_01_P009716	NR3C1 nuclear receptor subfamily 3 group C member 1 [*Homo sapiens* (human)]	-0.875572243	1.743903636	0.14867918	0.177589015	6.37E-06
A_01_P007215	CALN1 calneuron 1 [*Homo sapiens* (human)]	1.426402204	0	0	0	6.64E-06
A_01_P018202	CABP7 calcium binding protein 7 [*Homo sapiens* (human)]	1.778131921	0	0	0	6.73E-06
A_01_P006700	HCAR1 hydroxycarboxylic acid receptor 1 [*Homo sapiens* (human)]	1.578594952	0	0	0	6.78E-06
A_01_P009426	mitochondrial ribosomal protein S27 [Source:HGNC Symbol;Acc:HGNC:14512] [ENSMMUT00000070559]	1.802204642	0	0	0	7.88E-06
A_01_P005663	TRIOBP TRIO and F-actin binding protein [*Homo sapiens* (human)]	1.679785677	0	0	0.087840967	1.03E-05
A_01_P014991	GRK6 G protein-coupled receptor kinase 6 [*Homo sapiens* (human)]	1.245720233	0	0	0	1.09E-05
A_01_P018007	PREDICTED: Macaca mulatta leucine rich repeat and Ig domain containing 2 (LINGO2), mRNA [XM_002800071]	1.39474713	0	0	0	1.33E-05
A_01_P002698	FZD4 frizzled class receptor 4 [*Homo sapiens* (human)]	-2.149651068	1.421525723	-0.049240965	0.266166734	1.35E-05
A_01_P008315	ADAM metallopeptidase with thrombospondin type 1 motif 2 [Source:HGNC Symbol;Acc:HGNC:218] [ENSMMUT00000003541]	-1.846055929	0	0	0	1.43E-05
A_01_P015759	PREDICTED: Macaca mulatta DnaJ (Hsp40) homolog, subfamily B, member 11 (DNAJB11), mRNA [XM_001091858]	-0.959880885	1.615331811	1.012488459	0.308243661	1.53E-05
A_01_P018201	ANG angiogenin [*Homo sapiens* (human)]	-2.182916655	1.43747262	-1.930852499	-0.837917215	1.61E-05
A_01_P008576	PREDICTED: Macaca mulatta chemokine (C-X-C motif) ligand 12 (CXCL12), transcript variant X3, mRNA [XM_015146894]	0.041080614	3.971054733	0.682998768	0	1.62E-05
A_01_P002720	CNIH4 cornichon family AMPA receptor auxiliary protein 4 [*Homo sapiens* (human)]	-0.7668468	1.498210563	0.527656269	0.574219313	1.81E-05
A_01_P009023	PREDICTED: Macaca mulatta insulin-like growth factor binding protein 7, transcript variant 4 (IGFBP7), mRNA [XM_001083041]	-1.481873816	4.023203989	1.021473549	1.006494796	1.81E-05
A_01_P008865	GRK5 G protein-coupled receptor kinase 5 [*Homo sapiens* (human)]	1.135201541	0	0	0	2.01E-05

Supplemental Figure 1. **Clinical markers of SIVΔGY co-infection and *Mtb*/CD4R1 administration.** All animals were monitored for clinical signs of disease. *Mtb* CDC1551-infected LTBI (n=10, shown in blue), *Mtb*/SIVmac239 co-infected non-reactivators (n=7, shown in teal), *Mtb*/SIVmac239 co-infected reactivators (n=8, shown in yellow), *Mtb*/SIVΔGY co-infected (n=5, shown in pink), and *Mtb*/CD4R1-administered NHPs (n=8, shown in red). These included (A) serum C-reactive protein (CRP), which was measured weekly. (B) Bacterial burden was measured once every four weeks beginning at 1 week pre-infection with *Mtb* CDC1551. Bacterial burden was measured at necropsy per gram of tissue plated of (C) spleen, (D) liver, and (E) kidneys. *P < 0.05; **P < 0.01; ***P < 0.001; ****P <0.0001, one-way ANOVA with Tukey's multiple testing correction. Data represent mean ± SEM.

Supplementary Figure 1.

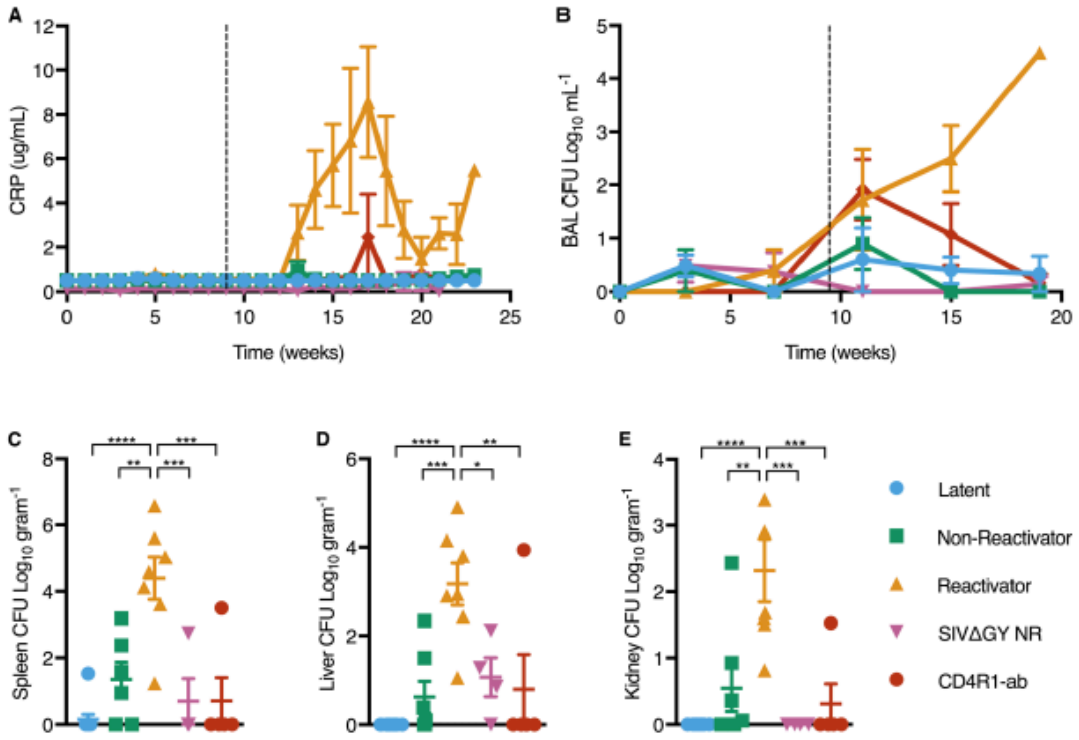

Supplementary Figure 2. Total CD4⁺ T cell depletion. CD4⁺ T cells were quantified by flow cytometric analysis from different tissues collected from rhesus macaques that were *Mtb* CDC1551-infected LTBI (n=10, shown in blue), *Mtb*/SIVmac239 co-infected non-reactivators (n=7, shown in teal), *Mtb*/SIVmac239 co-infected reactivators (n=8, shown in yellow), *Mtb*/SIVΔGY co-infected (n=5, shown in pink), and *Mtb*/CD4R1-administered (n=8, shown in red). CD4⁺ T cells were quantified and reported per 10,000

lymphocyte+ singlet cells in the (A) whole blood and in the (B) BAL every four weeks beginning at week 7 post-*Mtb* infection/week -2 prior to SIV co-infection. SIV-coinfection was performed at week 9 post-*Mtb* for selected groups, designated by the dotted line. CD4+ T cells were also quantified at necropsy in the (C) whole blood, (D) BAL, and (E) lungs. *P < 0.05; **P < 0.01; ***P < 0.001; ****P <0.0001, one-way ANOVA with Tukey's multiple testing correction. Data represent mean ± SEM.

Supplementary Figure 2.

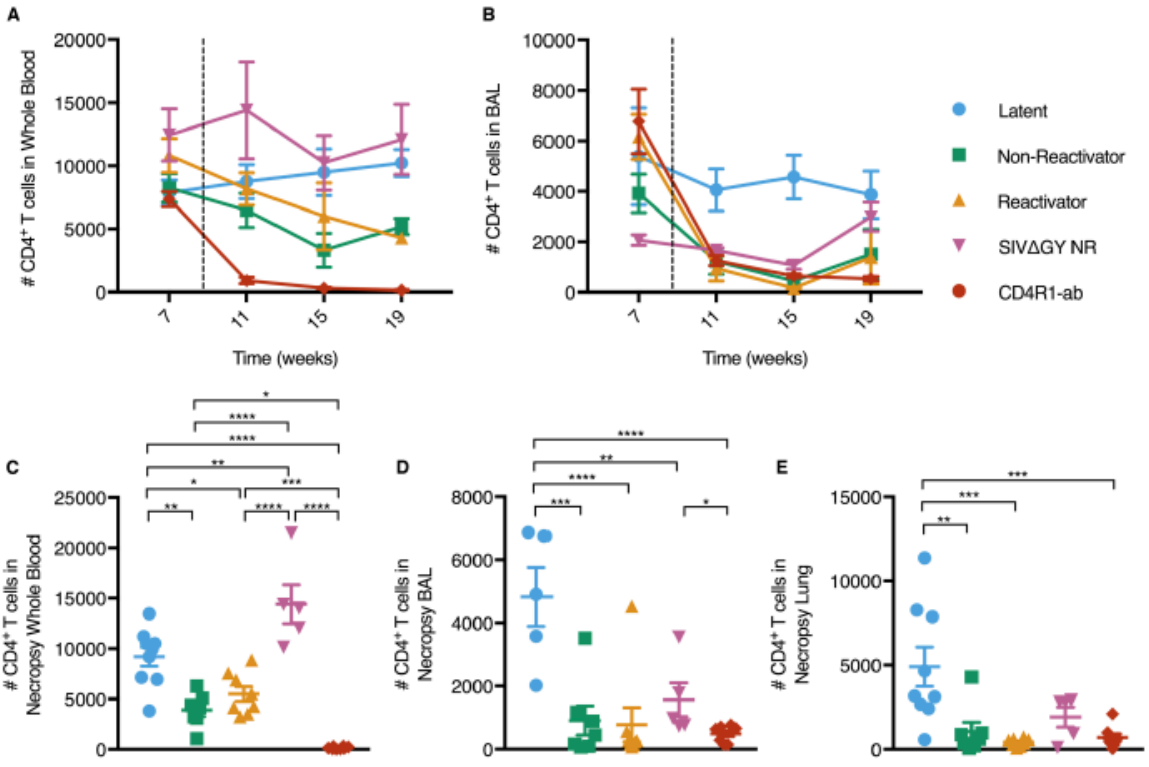

Supplementary Figure 3. Necropsy Lung CD4⁺ and CD8⁺ T cells reflect no proportional shifts following SIVmac239-coinfection or CD4 antibody-mediated depletion. Shown in all figures are the proportion of T cell sub-populations, naïve vs. effector vs. memory, in the CD4⁺ and CD8⁺ T cell compartments. At necropsy, the proportion of residual effector (CD95⁺CD28⁻, shown as circles), memory (CD95⁺CD28⁺, shown as squares), and naïve (CD95⁻CD28⁺, shown as upward triangles) (A) CD4⁺ T cells and (B) CD8⁺ T cells in the lungs did not significantly differ between LTBI (n=10, shown in blue) and SIVmac239-coinfected NHPs (n=15, shown in black) or NHPs administered CD4R1 (n=8, shown in red). *P < 0.05; **P < 0.01; ***P < 0.001; ****P <0.0001, two-way ANOVA with Tukey's multiple testing correction. Data represent mean ± SEM.

Supplementary Figure 3.

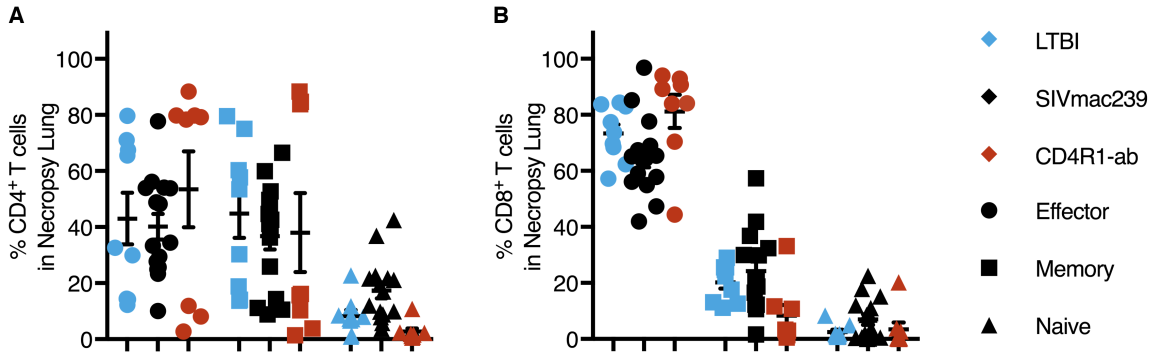

Supplementary Figure 4. Cytokine responses following $CD4^+$ T cell depletion due to SIV co-infection and CD4R1-administration. At week 15 post-*Mtb* infection and after 6 weeks of SIV-coinfection or antibody-mediated $CD4^+$ T cell depletion, the quantities of cytokines were measured in the plasma and BAL supernatant using Luminex analysis. Plasma and BAL supernatant were analyzed from *Mtb* CDC1551-infected LTBI (n=4, shown in blue), *Mtb*/SIVmac239 co-infected non-reactivators (n=3, shown in teal), *Mtb*/SIVmac239 co-infected reactivators (n=3, shown in yellow), *Mtb*/SIVΔGY co-infected (n=5, shown in pink), and *Mtb*/CD4R1-administered NHPs (n=4, shown in red). The concentration of IFN-γ was measured in (A) plasma and (B) BAL supernatant. The concentration of (C) CXCL9 was measured in the plasma. The concentration of (D) CXCL13, (E) Eotaxin, (F) I-TAC, and (G) IL-6 was measured in BAL supernatant. The concentration of (H) IL-8 and (I) MIP-1β was measured in plasma. The concentration of (K) SDF-1α was measured in BAL supernatant. *$P < 0.05$; **$P < 0.01$; ***$P < 0.001$; ****$P < 0.0001$, one-way ANOVA with Tukey's multiple testing correction. Data represent mean ± SEM.

Supplementary Figure 4.

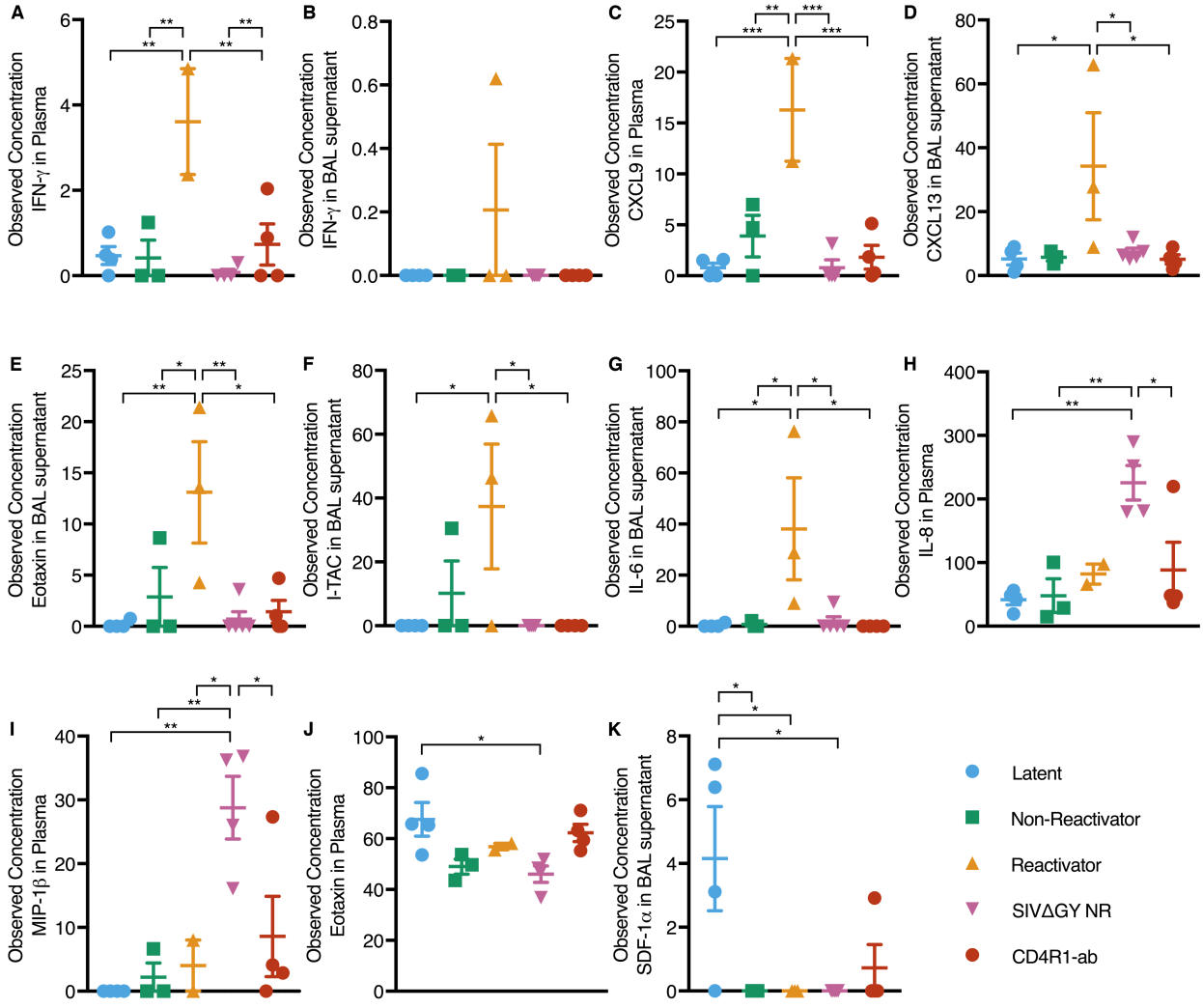

Supplementary Figure 5. Activation of CD8⁺ T cells is increased in reactivators compared to CD4R1-administered NHPs. CD8⁺ T cell expression of HLA-DR in the lungs at necropsy was measured using flow cytometric analysis (F) and co-expression of markers of migration (CCR5 and CCR7), activation (CD69), and apoptosis (PD-1) were measured in the (G) HLA-DR⁺ and (H) HLA-DR⁻ T cell population. *P < 0.05; **P < 0.01; ***P < 0.001; ****P <0.0001, multiple T-tests with Holm-Sidak method for multiple comparison correction. Data represent mean ± SEM.

Supplementary Figure 5.

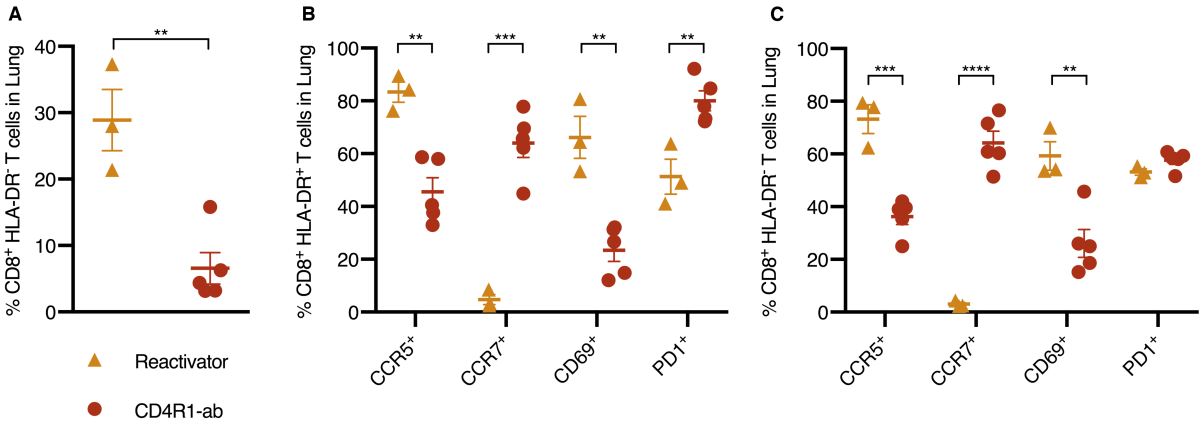

References:

1. Mehra S, Golden NA, Dutta NK, Midkiff CC, Alvarez X, Doyle LA, et al. Reactivation of latent tuberculosis in rhesus macaques by coinfection with simian immunodeficiency virus. *J Med Primatol.* 2011;40(4):233-43.
2. Mehra S, Golden NA, Stuckey K, Didier PJ, Doyle LA, Russell-Lodrigue KE, et al. The Mycobacterium tuberculosis stress response factor SigH is required for bacterial burden as well as immunopathology in primate lungs. *J Infect Dis.* 2012;205(8):1203-13.
3. Mehra S, Alvarez X, Didier PJ, Doyle LA, Blanchard JL, Lackner AA, et al. Granuloma correlates of protection against tuberculosis and mechanisms of immune modulation by Mycobacterium tuberculosis. *J Infect Dis.* 2013;207(7):1115-27.
4. Kaushal D, Foreman TW, Gautam US, Alvarez X, Adekambi T, Rangel-Moreno J, et al. Mucosal vaccination with attenuated Mycobacterium tuberculosis induces strong central memory responses and protects against tuberculosis. *Nat Commun.* 2015;6:8533.
5. Mehra S, Foreman TW, Didier PJ, Ahsan MH, Hudock TA, Kissee R, et al. The DosR Regulon Modulates Adaptive Immunity and is Essential for M. tuberculosis Persistence. *Am J Respir Crit Care Med.* 2015.
6. Foreman TW, Mehra S, LoBato DN, Malek A, Alvarez X, Golden NA, et al. CD4+ T-cell-independent mechanisms suppress reactivation of latent tuberculosis in a macaque model of HIV coinfection. *Proc Natl Acad Sci U S A.* 2016;113(38):E5636-44.
7. Kumar NA, McBrien JB, Carnathan DG, Mavigner M, Mattingly C, White ER, et al. Antibody-Mediated CD4 Depletion Induces Homeostatic CD4+ T Cell Proliferation without Detectable Virus Reactivation in Antiretroviral Therapy-Treated Simian Immunodeficiency Virus-Infected Macaques. *J Virol.* 2018;92(22).
8. Micci L, Alvarez X, Iriele RI, Ortiz AM, Ryan ES, McGary CS, et al. CD4 depletion in SIV-infected macaques results in macrophage and microglia infection with rapid turnover of infected cells. *PLoS Pathog.* 2014;10(10):e1004467.
9. Dutta NK, Mehra S, Didier PJ, Roy CJ, Doyle LA, Alvarez X, et al. Genetic requirements for the survival of tubercle bacilli in primates. *J Infect Dis.* 2010;201(11):1743-52.
10. Gautam US, Foreman TW, Bucsan AN, Veatch AV, Alvarez X, Adekambi T, et al. In vivo inhibition of tryptophan catabolism reorganizes the tuberculoma and augments immune-mediated control of Mycobacterium tuberculosis. *Proc Natl Acad Sci U S A.* 2017.
11. Foreman TW, Veatch AV, LoBato DN, Didier PJ, Doyle-Meyers LA, Russell-Lodrigue KE, et al. Nonpathologic Infection of Macaques by an Attenuated Mycobacterial Vaccine Is not Reactivated in the Setting of HIV Co-Infection. *Am J Pathol.* 2017.
12. Phillips BL, Mehra S, Ahsan MH, Selman M, Khader SA, and Kaushal D. LAG3 expression in active Mycobacterium tuberculosis infections. *Am J Pathol.* 2015;185(3):820-33.
13. Kuroda MJ, Sugimoto C, Cai Y, Merino KM, Mehra S, Arainga M, et al. High Turnover of Tissue Macrophages Contributes to Tuberculosis Reactivation in Simian Immunodeficiency Virus-Infected Rhesus Macaques. *J Infect Dis.* 2018.

14. Li Q, Skinner PJ, Duan L, and Haase AT. A technique to simultaneously visualize virus-specific CD8+ T cells and virus-infected cells in situ. *Journal of visualized experiments : JoVE.* 2009(30).
15. Mehra S, Pahar B, Dutta NK, Conerly CN, Philippi-Falkenstein K, Alvarez X, et al. Transcriptional reprogramming in nonhuman primate (rhesus macaque) tuberculosis granulomas. *PLoS One.* 2010;5(8):e12266.
16. Dutta NK, Mehra S, Martinez AN, Alvarez X, Renner NA, Morici LA, et al. The stress-response factor SigH modulates the interaction between Mycobacterium tuberculosis and host phagocytes. *PLoS One.* 2012;7(1):e28958.